Journal of Materials Science: Materials in Electronics (2019) 30:13151–13157
https://doi.org/10.1007/s10854-019-01678-2

Investigation of the structural, morphological and luminescence properties of $MgAl_2O_4$:Cr^{3+} nano powders

Yan Hao[1] · Kaipeng Wu[1]

Received: 5 March 2019 / Accepted: 10 June 2019 / Published online: 18 June 2019

Abstract
Cr^{3+} doped $MgAl_2O_4$ nano powders were prepared by the Pechini-type sol–gel process. Comprehensive analysis for the $MgAl_{2-x}O_4$:xCr^{3+}($0 \le x \le 0.05$) nano crystalline was performed using X-ray Diffraction, Fourier Transform Infrared Spectroscopy, Field Emission Scanning Electron Microscope, Diffuse Reflectance Spectra, Excitation and Emission Spectra. The powders calcined at 1100 °C were spherical with the average particle size of 90 nm, which were suitable for the preparation of the transparent ceramics. The crystal field, electron-vibration coupling and energy levels splitting of $MgAl_2O_4$: Cr^{3+} were discussed. The Cr^{3+} was suited in a strong crystal field, and the value of Dq/B = 3.9. At 457 nm excitations, the characteristic zero phonon lines appeared at 690 nm with the FWHM about 8 nm. The quenching concentration of Cr^{3+} was about 0.04.

1 Introduction

Recently, $MgAl_2O_4$ spinel has received many attentions because of its stable structure, high thermal shock resistance, high resistance against chemical attacks and transparency in a wide spectral range, etc. $MgAl_2O_4$ spinel belongs to the $A^{2+}B_2{}^{3+}O_4$ structure of the cubic space group Fd3m, and one cubic cell has eight $MgAl_2O_4$ units. The Mg^{2+} and O^{2-} constituted the tetrahedral coordination with full T_d symmetry (1/8 of the available site A); Al^{3+} has octahedral coordination with D_{3d} symmetry (1/2 of the available site B). Such behaviors make it be considered as a good host of holding a great deal of divalent and trivalent cations in solid-state solution [1, 2]. The transition-metal ions doped in $MgAl_2O_4$ form a colorful group of phosphor materials [3], such as doped with Co^{2+} [4, 5], Cr^{3+} [6, 7], Ti^{4+} [8, 9] and Mn^{2+} [10, 11]. In recent years, Cr^{3+} doped in $MgAl_2O_4$ has been studied widely, and the reports revealed that $MgAl_2O_4$:Cr^{3+} is a new potential candidate as laser applications, scintillators, biomarkers for in vivo imaging and sensing [12–15].

The photoluminescence properties of Cr^{3+} are highly relative with the crystal field strength and may produce the emission either from the exited state ^2E or $^4T_2$ to ground state $^4A_2$. There are two types of materials: one is due to the $^4T_2$–$^4A_2$ spin-allowed transition in low-field materials and the other is assigned to the ^2E–$^4A_2$ spin forbidden transition (R-line) in high-field materials [16]. Usually, its excitation spectrum is a broad band from 400 to 660 nm and composed of two excited bands derived from the transitions of Cr^{3+}, the $^4A_2$–$^4T_1$(~ 420 nm) and $^4A_2$–$^4T_2$(~ 540 nm) transition [17–19]. Since spinels can be used for laser materials, scintillators and sensing, it is necessary to further to understand the effect of the crystal field on the photoluminescence behavior of Cr^{3+}. In this work, $MgAl_{2-x}O_4$:xCr^{3+} ($0 \le x \le 0.05$) were synthesized through the Pechini-type sol–gel process, and their structure, morphology, photoluminescence and the crystal field parameters were investigated.

2 Experimental

2.1 Synthesis of $MgAl_2O_4$:Cr^{3+} nanopowders

All samples were synthesized through the Pechini-type sol–gel process. The starting materials were $Mg(NO_3)_2{\cdot}6H_2O$ (AR, 99.5%), $Al(NO_3)_3{\cdot}9H_2O$ (AR, 99.0%), $Cr(NO_3)_3{\cdot}9H_2O$ (AR, 99.0%), citric acid (CA, AR, 98%) and ethylene glycol (EG). Stoichiometric ratio of the starting materials (Mg:Al:CA:EG = 1:2:3:6) was dissolved in ethanol and water. And the solution was adjusted to the pH of 4 with NH_4OH. Then the solution was heated to 90–100 °C till forming the sol, and the whole process were accompanied

✉ Yan Hao
haoy420@163.com

[1] State Key Laboratory for Environment-Friendly Energy Materials, Southwest University of Science and Technology, Mianyang 621010, China

by magnetic stirring. The sol was left in the air for about 1 day, and then was dried in an oven at 120 °C for 20 h. Finally, the dried gel was ground to powders and calcined at 600–1100 °C for 3 h.

2.2 Characterization

The XRD patterns were measured by Rigaku DMAX1400 X-ray diffractometer with Cu Kα (λ = 0.15406 nm) incident radiation. The morphologies were examined by Tescan MAIA3 ultra high-resolution FESEM. The FTIR spectra were carried out by Nicolet 5700 Fourier transformations infrared spectrometer with standard KBr disk technique. The diffuse reflection spectra were performed by Shimadzu Solidspec-3700 UV–VIS-NIR spectrophotometer. The excitation and emission spectra were examined by Perkin Elmer LS 55 fluorescence spectrophotometer.

3 Results and discussion

3.1 Structure

The XRD patterns were shown in Fig. 1. It confirmed that the single phase of $MgAl_2O_4$ were present until the temperature arrived at 700 °C. The intensity of diffraction peak improved evidently as the increasing of calcination temperatures, and this was caused by the growth of the crystallinity. The lattice parameters and crystallite size can be calculated through Bragg diffraction and Scherrer's equation, and the calculation results were shown in Fig. 3f. It's evident that the crystallite size grew slowly below 900 °C and increased obviously after that. And the result was similar to the previous report [13, 18].

The FTIR of $MgAl_{1.96}O_4$:$0.04Cr^{3+}$ calcined at 700 °C to 1100 °C were shown in Fig. 2. The spectra exhibited four major transmittance bands of 548 cm^{-1}, 707 cm^{-1}, 1406 cm^{-1} and 1636 cm^{-1}. The bands observed at 548 cm^{-1} and 707 cm^{-1} were corresponded to octahedral and tetrahedral Al–O bonds of the regular spinel structure [17, 20]. It's clear that the bands shifted to lower wavenumbers and their boundary became clearer about the increase in calcination temperatures. This was identified with the results of Fig. 1. The band of 1407 cm^{-1} was due to the stretching vibration of CO_3^{2-} [1, 20]. It revealed that some metal carbonates existed on the samples calcined at 800 °C and it became weak as the calcination temperatures increasing. The metal carbonates disappeared until the calcination temperatures arrived at 1100 °C. The transmittance bands at 1636 cm^{-1} corresponded to H–O–H bending vibrations. Besides, the spectra showed three weak bands of 1050 cm^{-1}, 1083 cm^{-1} and 1517 cm^{-1}. The C–O stretching vibration was at 1050 cm^{-1}, and it disappeared above 1000 °C. The Mg–O–C bending resonated with 1083 cm^{-1} [20]. The band of 1517 cm^{-1} should be the N–O stretching of nitrate group [20], and it disappeared when calcination temperatures were above 700 °C.

3.2 Morphology

The FESEM micrographs and particle sizes distribution histogram of $MgAl_{1.96}O_4$: $0.04Cr^{3+}$ samples were shown in Fig. 3 It's clear that the powders calcined below 1000 °C were near-spherical and uniform. The average particle size was 20–30 nm below 900 °C and then increased evidently after 900 °C. It was in accordance with the results of the XRD spectra. The samples calcined at 1100 °C were spherical and the average particle size was 90 nm. Nam [21] reported that the spherical-spinel powder is helpful

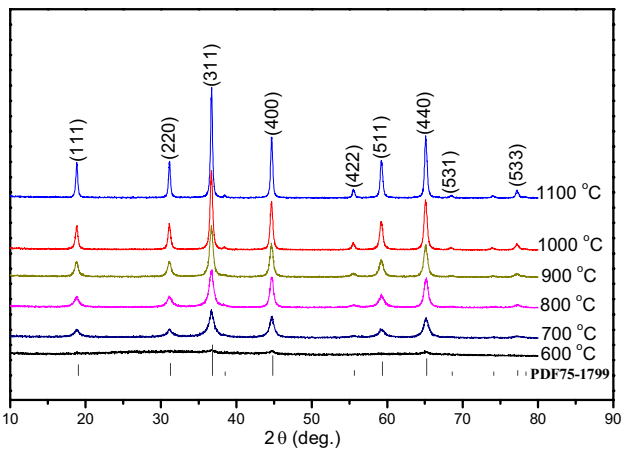

Fig. 1 XRD patterns of $MgAl_{1.96}O_4$:$0.04Cr^{3+}$ calcined at different temperatures

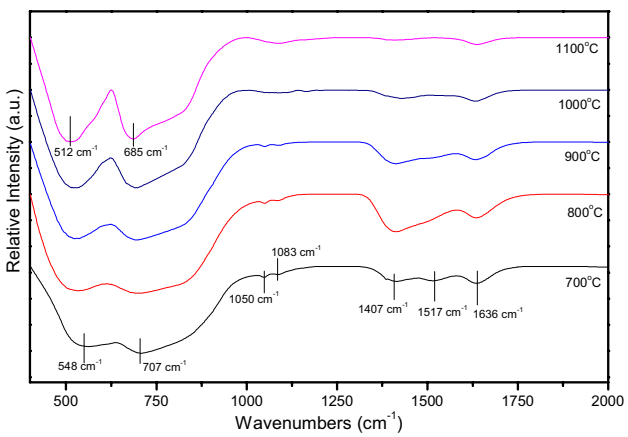

Fig. 2 FTIR spectra of $MgAl_{1.96}O_4$:$0.04Cr^{3+}$calcined at different temperatures

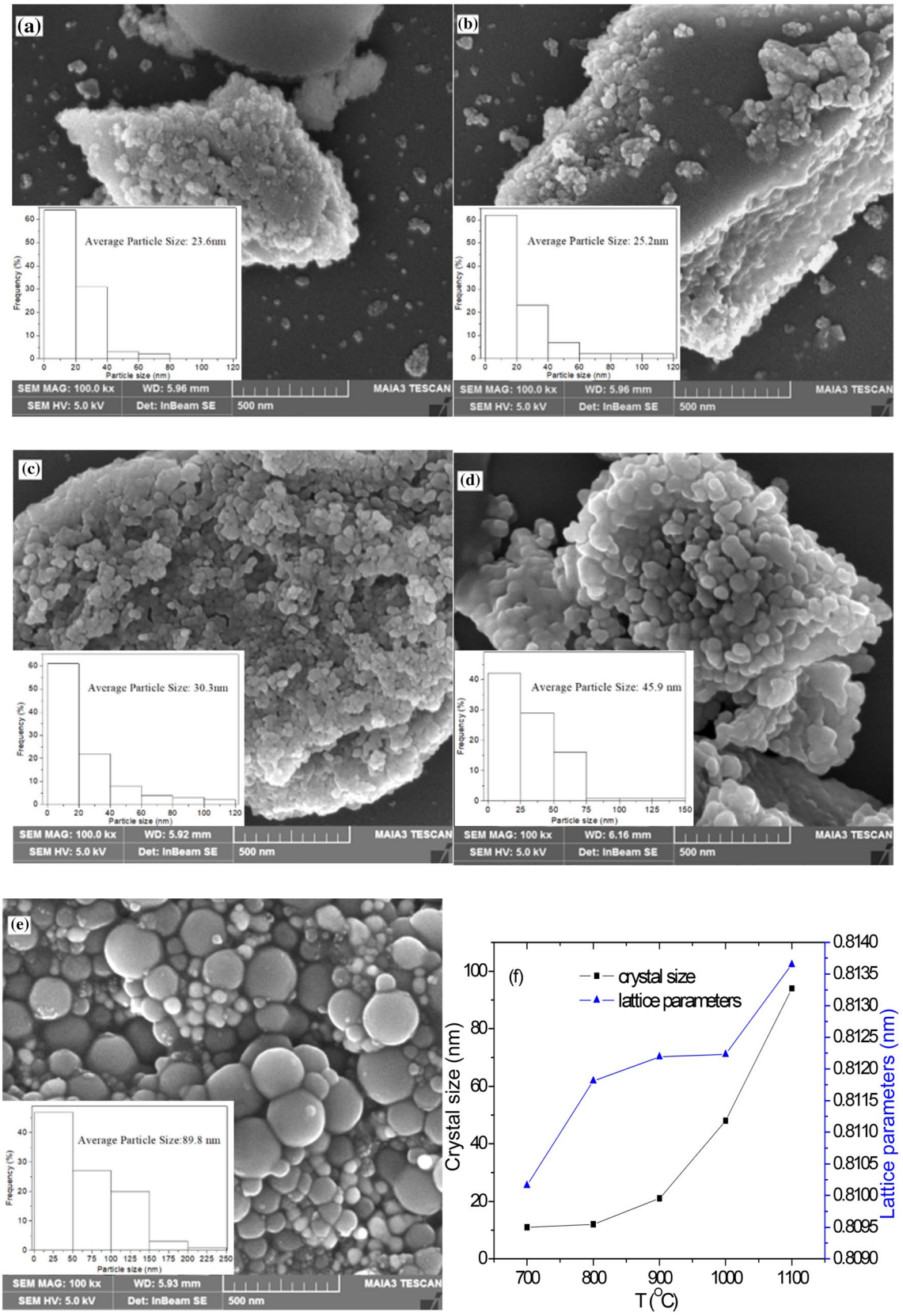

Fig. 3 FESEM,particle sizes distribution histogram, crystallite size and lattice parameters of $MgAl_{1.96}O_4$:$0.04Cr^{3+}$, **a** 700 °C; **b** 800 °C; **c** 900 °C; **d** 1000 °C; **e** 1100 °C; **f** crystallite size and lattice parameters

for high densification and smaller grain size of transparent $MgAl_2O_4$ ceramics. Accordingly, the $MgAl_2O_4$:Cr^{3+} nano powder obtained from the Pechini-type sol–gel process is suitable for the preparation of the transparent $MgAl_2O_4$:Cr^{3+} ceramics.

3.3 Photoluminescence properties

The excitation and emission spectra of $MgAl_{1.96}O_4$:$0.04Cr^{3+}$ calcined at different temperatures were similar and the sample calcined at 1100 °C had the highest luminescent intensity. The excitation ($\lambda_{em}=522$, 574 and 694 nm) and emission ($\lambda_{ex}=250$, 300 and 460 nm) spectra of $MgAl_{1.96}O_4$:$0.04Cr^{3+}$ calcined at 1100 °C were shown in Fig. 4. The excitation spectrum ($\lambda_{em}=522$ nm) was a broad excitation band centered around 236 nm, which could be attributed to the host and the charge transferred band of Cr^{3+}–O^{2-} [6, 13]. The excitation spectrum ($\lambda_{em}=574$ nm) included a broad band centered around 236 nm, 250 nm and 300 nm. These excited bands were also due to the host and the charge transfer band of Cr^{3+}–O^{2-}. The excitation spectrum ($\lambda_{em}=690$ nm) included a broad band centered around 250 nm and a narrow band of the maximum at 457 nm. The former was due to the host and the charge transferred band of Cr^{3+}–O^{2-}, and the latter was assigned to the spin-forbidden transition of $^4A_2$–$^2T_2$ [15, 19].

The emission spectra ($\lambda_{ex}=250$ nm) included a broad band centered around 425 nm (23,529 cm^{-1}), 461 nm (21,692 cm^{-1}), 498 nm (20,080 cm^{-1}), 522 nm (19,157 cm^{-1}) and 690 nm (14,493 cm^{-1}), and their attributions were also shown in Fig. 4. The emission bands of 425 nm (23,529 cm^{-1}), 461 nm (21,692 cm^{-1}) were assigned to the transition of $^4T_1$–$^4A_2$ and $^2T_2$–$^4A_2$, respectively. It's known that the $^4A_2$–$^4T_2$ transition was a broad band of 480–560 nm [17–19], and there existed an obvious splitting in Fig. 4b. Brik [16] reported that stronger crystal field implied larger splitting of the orbital triplets, especially for the $^4T_2$ state. It can be concluded that Cr^{3+} was suited in a stronger crystal field and the emission bands centered around 488 nm, 498 nm, 508 nm, 522 nm, 537 nm and 548 nm were attributed to the transitions of the splitting $^4T_2$ state to the ground state $^4A_2$. The emission bands of 574 nm (17,421 cm^{-1}), 597 nm (16,750 cm^{-1}) and 622 nm (16,077 cm^{-1}) were assigned to the transition $^2T_1$–$^4A_2$. It also can be concluded that there existed an obviously splitting of the $^2T_1$ states. The emission band of 690 nm was the characteristic zero phonon line (ZPL, R-line) ascribed to the ^2E–$^4A_2$ transition of Cr^{3+}, and the weak emission band around it were the multi phonon side of Cr^{3+} bands of either side of the ZPL [13–15]. It's clear that the emission of the $^4T_2$–$^4A_2$ and ^2E–$^4A_2$ transitions became weaker and the emission of the $^2T_1$–$^4A_2$ transition got stronger when the excitation wavelength was 300 nm. And excited at 457 nm, it only showed the ^2E–$^4A_2$ transition with the FWHM about 8 nm. The chromaticity coordinates were shown in the inset of Fig. 4b.

The emission intensities ($\lambda_{ex}=457$ nm) as calcination temperatures and the concentration of Cr^{3+} were displayed in the inset of Fig. 4a. It's expected that the emission intensity increased as calcination temperatures, which was owned to the crystallization of the sample. It's also evident that the quenching concentration of Cr^{3+} was $x=0.04$. In this work, a higher quenching concentration was obtained comparing with the previous reports [13, 19], which could be attributed to the better molecular homogeneity and monodisperse nanoparticles obtained from the Pechini-type sol–gel process.

Brik et al. [16] presented that the emissions of Cr^{3+} ions depended on the strength of the crystal field: the low-field materials ($^4T_2$–$^4A_2$ spin-allowed transition) and the high-field materials (^2E–$^4A_2$ spin forbidden transition). But in this work ($\lambda_{ex}=457$ nm), the $^4T_2$–$^4A_2$ and ^2E–$^4A_2$ transitions appeared simultaneously. And the obvious $^2T_1$–$^4A_2$ transition was observed at $\lambda_{ex}=300$ nm. It seemed that Cr^{3+} was suited in complicated surroundings. The diffuse reflectance spectra of $MgAl_{2-x}O_4$:xCr^{3+} ($0\le x\le 0.05$) were also measured and shown in Fig. 5. The diffuse reflectance spectra were composed of three broad bands centered around 270 nm, 369 nm and 543 nm. The band of 270 nm was ascribed to the $MgAl_2O_4$ host; meanwhile the charge transfer band of Cr^{3+}–O^{2-} was also in this region [12]. The band of 369 nm (27,100 cm^{-1}) was assigned to $^4A_2$–$^2A_1$ transitions of Cr^{3+}, and its shoulder band included the $^4A_2$–$^4T_1$ and $^4A_2$–$^2T_2$ transitions [16, 22]. The absorption band centered on 543 nm (18,416 cm^{-1}) was due to the $^4A_2$–$^4T_2$ transitions of Cr^{3+}. The relative weak band appeared at 667 nm (14993 cm^{-1}) was originated from $^4A_2$–$^2T_1$ transitions of Cr^{3+}. According to the excitation, emission spectra and the diffuse reflectance spectra, the energy level diagram of Cr^{3+} in nano-$MgAl_2O_4$ powders can be obtained and shown in the inset of Fig. 5. Meanwhile, basing on Tanabe–Sugano theory, the experienced crystal field parameters D_q, the Racah parameters B and C can be calculated by the energies of these transitions [23–25]. The energies of $^4A_2$–$^4T_2$, $^4A_2$–$^4T_1$ and ^2E–$^4A_2$ transitions were ν_1 (543 nm, 18,416 cm^{-1}), ν_2 (425 nm, 23,529 cm^{-1}) and ν (690 nm, 14,493 cm^{-1}) respectively. D_q, B and C can be calculated by the following formula:

$$10D_q = \nu_1 \tag{1}$$

$$B = \frac{(2\nu_1 - \nu_2)(\nu_2 - \nu_1)}{(27\nu_1 - 15\nu_2)} \tag{2}$$

$$9B + 3C = \nu \tag{3}$$

Consequently, D_q was about 1842 cm^{-1}, B was about 471 cm^{-1} and C was about 3418 cm^{-1}. The value of Dq/B

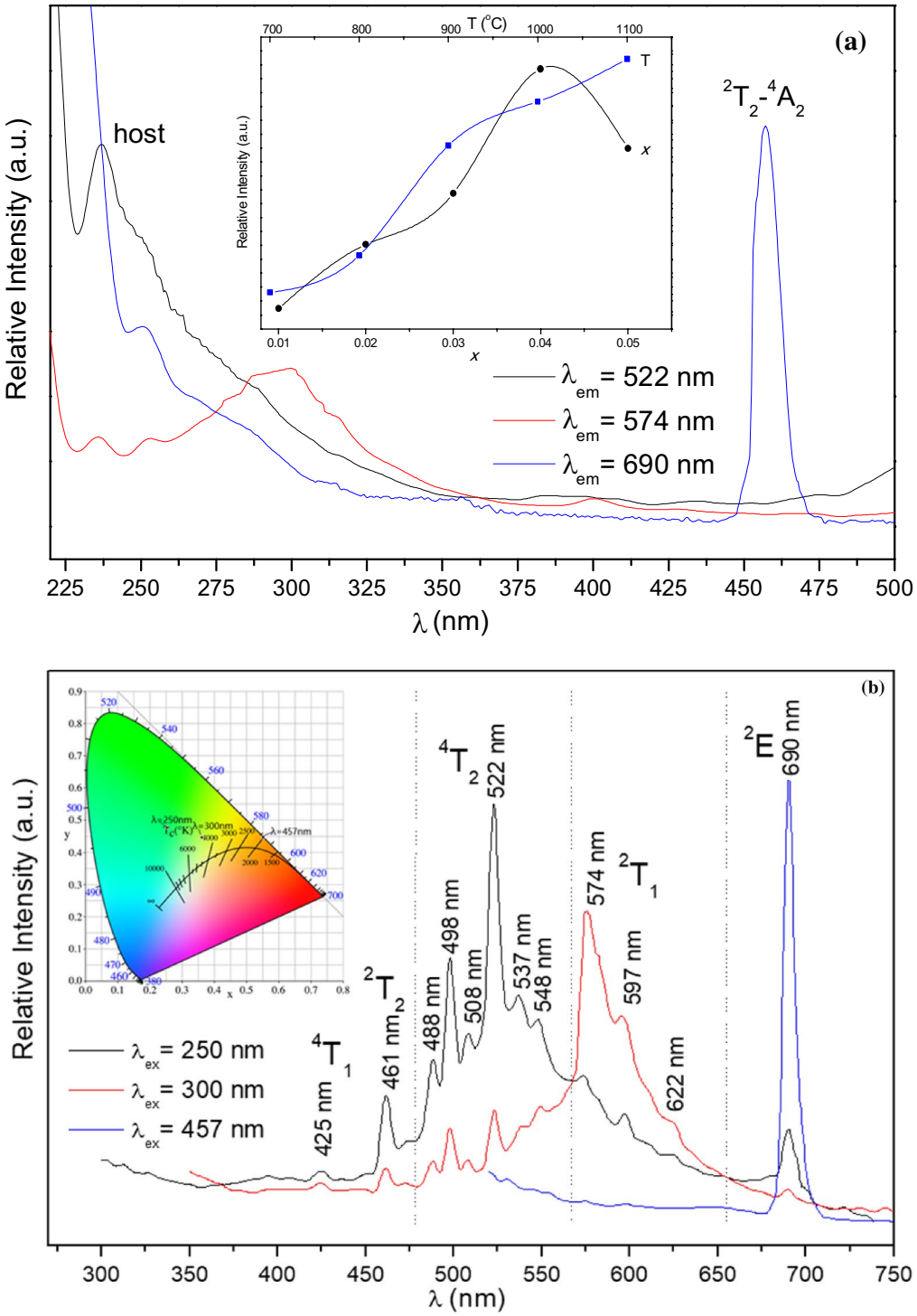

Fig. 4 Excitation (**a**) and emission (**b**) spectra of $MgAl_{1.96}O_4$:0.04Cr^{3+} calcined at 1100 °C, the inset in **a**: emission intensity (λ_{ex} = 457 nm) as calcination temperatures and Cr^{3+} concentration, and the inset in **b**: chromaticity coordinates

was 3.9. It's higher than the previous reported to be 3–3.5 [12, 13, 17]. And it is accordance with the results of the emission spectra, the obvious energy level splitting of $^4T_2$ and $^2T_1$ state. Comparing with the previous reports [16–19], the well-known excited bands derived from the $^4A_2$–$^4T_1$(~420 nm) and $^4A_2$–$^4T_2$(~540 nm) transition of Cr^{3+} were not detected in this work. Brik [16] also reported that the energy excitation band ($^4A_2$–$^4T_1$ transition) is explained by a well-known effect of "intensity borrowing", when the $^4T_1$ and $^2T_2$ state are mixed by spin–orbit coupling. But in

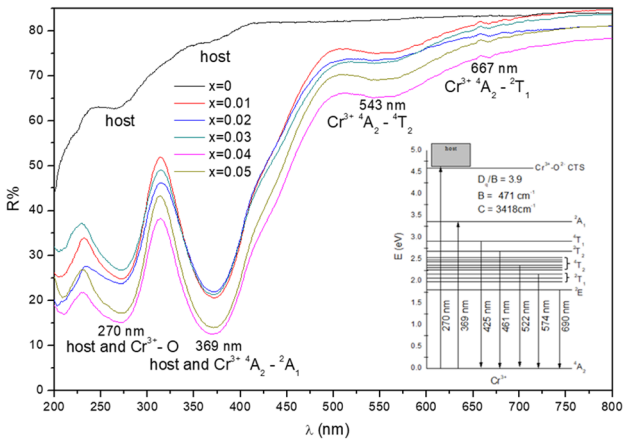

Fig. 5 Diffuse reflectance spectra of $MgAl_{2-x}O_4$: xCr^{3+} ($0 \le x \le 0.05$) calcined at 1100 °C, the inset was the energy level diagram of Cr^{3+}

Fig. 4b, the $^4T_1$–$^4A_2$ and $^2T_2$–$^4A_2$ transitions were separated evidently, which meant that the coupling between the $^4T_1$ and $^2T_2$ state were weak. It's also because that in this work Cr^{3+} ion was situated in a stronger crystal field.

4 Conclusion

Cr^{3+} doped $MgAl_2O_4$ nano powders were successfully synthesized through the Pechini-type sol–gel process. The results showed the $MgAl_2O_4$ spinel phase appeared when the temperature arrived at 700 °C, and the particle sizes were grown as calcinations temperatures increased. The results were accordance with the results of FESEM. The FESEM images also showed that the powders calcined at 1100 °C were spherical and the average particle size was about 90 nm. The study on the optical performance revealed that in the obtained $MgAl_2O_4$:Cr^{3+} nano powders, Cr^{3+} was suited in a high crystal field with the value of Dq/B = 3.9. The strong crystal field caused an obvious splitting of the $^4T_2$ and $^2T_1$ state, and the weak coupling between the $^4T_1$ and $^2T_2$ state. The $MgAl_2O_4$:Cr^{3+} nano powders showed different emissions at different excitations, broad band emission centered at 522 nm ($^4T_2$–$^4A_2$, λ_{ex} = 457 nm), broad band emission centered at 574 nm ($^2T_1$–$^4A_2$, λ_{ex} = 300 nm) and R-line emission centered at 690 nm (^2E–$^4A_2$, λ_{ex} = 457 nm). Comparing with previous reports, Cr^{3+} suited in a stronger crystal field and had a higher quenching concentration. The higher crystal field and the quenching concentration could be attributed to the better molecular homogeneity and monodisperse nanoparticles obtained from the Pechini-type sol–gel process.

Acknowledgements This work was supported by the National Natural Science Foundation of China (Grant No. 51802272) and the Longshan academic talent research support plan of Southwest University of Science and Technology (18LZXY02).

References

1. I. Ganesh, A review on magnesium aluminate ($MgAl_2O_4$) spinel: synthesis, processing and applications. Int. Mater. Rev. **58**, 63–112 (2013)
2. I. Omkaram, B. Vengala Rao, S. Buddhudu, Photoluminescence properties of Eu^{3+}: $MgAl_2O_4$ powder phosphor. J. Alloys Compd. **474**, 565–568 (2009)
3. K. Izumi, S. Miyazaki, S. Yoshida et al., Optical properties of 3*d* transition-metal-doped $MgAl_2O_4$ spinels. Phys. Rev. B **76**, 075111 (2007)
4. W. Luo, Y.B. Pan, C.Y. Li, H.M. Kou, J. Li, Fabrication and spectral properties of hot-pressed Co: $MgAl_2O_4$ transparent ceramics for saturable absorber. J. Alloys Compd. **724**, 45–50 (2017)
5. H.-Y. Lin, D. Sun, N. Copner, W.-Z. Zhu, Nd:GYSGG laser at 1331.6 nm passively Q-switched by a Co:$MgAl_2O_4$ crystal. Opt. Mater. **69**, 250–253 (2017)
6. V. Singh, R.P.S. Chakradhar, J.L. Rao, D.-K. Kim, Combustion synthesized MgAl2O4: Cr phosphors—An EPR and optical study. J. Lumin. **129**, 130–134 (2009)
7. E.S. Artemyeva, D.S. Barinov, F.M. Atitar, A.A. Murashkina, A.V. Emeline, N. Serpone, Luminescence of photoactivated pristine and Cr-doped $MgAl_2O_4$ spinel. Chem. Phys. Lett. **626**, 6–10 (2015)
8. J. Lim, Y. Kim, S. Kim, Y.K.S. Kang, Defects on the surface of Ti-doped $MgAl_2O_4$ nanophosphor. Nanoscale Res. Lett. **12**, 536 (2017)
9. J.H. Lim, B.N. Kim, Y. Kim, S. Kang, R.J. Xie, I.S. Chong, K. Morita, H. Yoshida, K. Hiraga, Non-rare earth white emission phosphor: Ti-doped $MgAl_2O_4$. Appl. Phys. Lett. **102**, 031104 (2013)
10. Toru Katsumata, Hiromasa Mitomi, Hijiri Nagayam et al., Compositional variations in optical characteristics of Mn doped spinel crystals. J. Cryst. Growth **468**, 387–390 (2017)
11. A.V. Mali, T.M. Wandre, K.R. Sanadi, A.S. Tapase, I.S. Mulla, P.P. Hankare, Synthesis, characterization and electrical properties of novel Mn substituted $MgAl_2O_4$ synthesized by sol-gel method. J. Mater. Sci. **27**, 613–619 (2016)
12. G.H. Sun, Q.L. Zhang, J.Q. Luo, Bulk crystal growth of Cr-doped $MgAl_2O_4$ spinel by Czochralski method and properties characterization. Mater. Chem. Phys. **204**, 277–281 (2018)
13. H.G. Shreekrishna Karthik, G. Samvit, S.G. Menon et al., Nanocrystalline $MgCrxAl_2$-xO_4: facile synthesis and thermal dependency of photoluminescence. Mater. Res. Bull. **94**, 513–519 (2017)
14. Y. Lu, Y. Linhua, B. Renjie, Z. Xianwei, W. Ligang, Growth and fluorescence temperature characteristics of Cr^{3+} doped $MgAl_2O_4$ single crystal optical fiber. J. Synth. Cryst. **46**, 1672–1677 (2017)
15. S.V. Motloung, B.F. Dejene, R.E. Kroon, O.M. Ntwaeaborwa, H.C. Swart, T.E. Motaung, The influence of Cr3+ concentration on the structure and photoluminescence of $MgAl_2O_4$:0.1% Eu^{3+}, x% Cr^{3+} ($0 \le x \le 0.15\%$) nanophosphor synthesized by sol-gel process. Optik **131**, 705–712 (2017)
16. M.G. Brik, J. Papan, D.J. Jovanović, M.D. Dramićanin, Luminescence of Cr^{3+} ions in $ZnAl_2O_4$ and $MgAl_2O_4$ spinels: correlation between experimental spectroscopic studies and crystal field calculations. J. Lumin. **177**, 145–151 (2016)
17. A.R. Molla, C.R. Kesavulu, R.P.S. Chakradhar et al., Microstructure, mechanical, thermal, EPR, and optical properties of $MgAl_2O_4$:Cr^{3+} spinel glass–ceramic nanocomposites. J. Alloys Compd. **583**, 498–509 (2014)

18. P. Głuchowski, R. Pa˛zik, D. Hreniak, W. Strek, Luminescence studies of Cr^{3+} doped $MgAl_2O_4$ nanocrystalline powders. Chem. Phys. **358**, 52–56 (2009)
19. Du Xinhua, Hai Tian, Shiyue Yao, Yumei Long, Bo Liang, Weifeng Li, Spectroscopic properties of $MgAl_{2-x}O4:xCr^{3+}$nanoparticles preparedby a high-temperature calcination method. Phys. B **478**, 17–21 (2015)
20. Worawut Nantharak, Worawat Wattanathana, Wantana Klysubun*et al*, Effect of local structure of Sm^{3+} in $MgAl_2O_4:Sm^{3+}$ phosphors preparedby thermal decomposition of triethanolamine complexes on theirluminescence property. J. Alloys Compd. **701**, 1019–1026 (2017)
21. Sangwoo Nam, Munkeun Lee, Byung-Nam Kim et al., Morphology controlled Co-precipitation method for nano structured transparent $MgAl_2O_4$. Ceram. Int. **43**, 15352–15359 (2017)
22. U. HåleniUs, G.B. Andreozzi, H. Skogby, Structural relaxation around Cr^{3+} and the red-green color change in the spinel (sensu stricto)-magnesiochromite ($MgAl_2O_4$-$MgCr_2O_4$) and gahnite-zincochromitem ($ZnAl_2O_4$-$ZnCr_2O_4$) solid-solution series. Am. Mineral **95**, 456–462 (2010)
23. S.G. Menon, D.N. Hebbar, S.D. Kulkarni, K.S. Choudhari, C. Santhosh, Facile synthesis and luminescence studies of nanocrystalline red emitting Cr: $ZnAl_2O_4$ phosphor. Mater. Res. Bull. **86**, 63–71 (2017)
24. S. Sugano, Y. Tanabe, H. Kamimura, *Multiplets of transition-metal ions in crystal* (Academic Press, New York, 1970)
25. Yuan Jianhui, Yang Changhu, Zhang Zhenhua, Yuan Xiaobo, Spectral characteristics and crystal field parameters of the Cr^{3+} doped $Cd_3Al_2Ge_3O_{12}$. Chinese Phys. Soc. **57**(8), 5272–5276 (2008)